INVESTIGATION OF TURBULENT WAKE-BOUNDARY
LAYER INTERACTION WITH INJECTION

T. I. SABRY*, N. I. I. HEWEDY**, M.H. EMBABY*** & A. A. ELBATAWY****

ABSTRACT

The present paper is concerned with experimental study of the interaction between a wake, with injection at its beginning, and a boundary layer. The wake is developed downstream a finite length and thickness plate inside an open-type wind tunnel test section while the boundary layer is developed over the wall of the test section. The measurements are carried out at Reynolds number 1.8×10^5 and injection to main stream velocity ratios (λ) of ($0 < \lambda < 0.7$). In the experiments the mean velocity profiles, the wall static pressure distribution and the local skin friction coefficient are measured. The results indicate that, for a certain velocity ratio, moving downstream from the trailing edge of the thick plate the wake decays while the boundary layer grows gradually. Also, the wake depth decreases, the wake width increases and the position of maximum velocity moves into the inner layer. On the other hand-at a certain distance from the trailing edge-as the velocity ratio increases the wall pressure coefficient, the momentum thickness Reynolds number and the shape factor decrease while the skin friction coefficient increases. Also-as the velocity ratio increases the rate of wake decay, the wake center line velocity and the wake width increase while the wake depth decreases.

INTRODUCTION

The study of the interaction between a developed turbulent wake downstream of a thick body and boundary layer with injection through a jet is very important for many practical engineering applications. Review of the previous work, on the turbulent wakes and jet-boundary interaction, may help such a study. The turbulent two dimensional incompressible wake of a thin plate has been studied experimentally in [1]. They have studied both symmetric and asymmetric cases of a wake. The results showed that for both symmetric and asymmetric wakes

* Professor, Head of Department & Vice Dean, ** Associate Professor, *** Lecturer, **** Demonstrator, Mechanical Power Engineering Department, Menoufia University, Shebin ElKom, EGYPT.

momentum thickness remains constant in the wake and the displacement thickness decreases down stream of the trailing edge approaching the value of momentum thickness. It was also found that for the symmetric wake the centre-line velocity obeys a logarithmic law. Turbulent wake behind an aerofoil with positive, negative and zero pressure gradient was studied experimentally by Heikal and Others [2]. The measurements showed that, positive pressure gradient slows the action of the wake and decreases the rate of wake decay compared with that of zero or negative pressure gradients. Experimental study of the plane turbulent wake behind an aerofoil with pressure gradient was carried out by Heikal and Others [3]. The results showed that for the same free stream velocity and distance from the trailing edge as the positive pressure gradient increases the wake width, the displacement and the momentum thickness increase while the total drag coefficient slightly decreases. Also as the negative pressure gradient increases the wake depth decreases sharply while wake width increases. Also, with increasing distance from the trailing edge, the displacement and momentum thicknesses decrease while the drag coefficient increases. The calculation of turbulent wakes were carried out by Chang and Others [4]. The velocity distribution, integral properties and Reynolds stresses were computed and compared with available measurements for wake flows. They concluded that, provided the cross-stream pressure gradients associated with wake curvatures are represented properly by the form of the momentum equation, the algebraic eddy viscosity approach is adequate for the wakes considered. An experimental and theoretical investigation of the interaction between the engine jet and the surrounding flow field with regard to the pressure drag on afterbodies were carried out by Zacharias [5]. He studied the influence of entrainment and plume effects of the jet on the afterbody pressure distribution and pressure drag. The experimental results indicated the dependence of the plume effect, the entrainment and the afterbody pressure drag on the jet parameters such as the free stream Mach number and the afterbody geometry. He used theoretical potential flow model to calculate the pressure drag on rotationally symmetric afterbodies. Comparison of the theoretical and experimental results showed good agreement.

Two dimensional turbulent offset jet boundary interaction were investigated theoretically and experimentally by Hoch, and Jiji [6]. The jet was discharged parallel to and offset from a solid wall in the presence of main free stream in the theoretical model. They used an integral solution coupled with an entrainment assumption to predict jet-boundary interaction to check the validity of their theoretical model. They carried out measurements in a low speed wind test section. They observed good agreement between experimental and theoretical predictions. The above review shows that the turbulent wake boundary layer interaction with injection have not been fully explored. The present paper is concerned with experimental study of the interaction between a wake, with injection at its beginning, and boundary layer.

EXPERIMENTAL SET-UP AND MEASURING TECHNIQUES:

The Experimental Apparatus:

The experiments were carried out in the test section of an open-type wind tunnel illustrated in Fig. 1. The upper wall of the

test section was provided with horizontally movable blocks to allow probe insertion into the test section. Forty pressure taps were drilled on the bottom wall at longitudinal distance of 20 mm a part. All the test section was manufactured from transparent perspex sheets with 12 mm thickness. The test model, shown in Fig. (1), consists of a thick plate with rounded trailing and leading edges. The trailing edge has 12 circular holes of 10 mm diameter at distance of 10 mm a part in the plane of symmetry of the cross section. The test model is made of painted smooth wood with the dimensions of 270 mm length, 300 mm width and height of 60 mm. It was provided with two layers of screens at a distance of 30 mm from the trailing edge to break down the secondary vortices and to reduce the turbulence of the blowing flow. The test model was placed in the plane of symmetry of the wind tunnel, parallel to the wall, and connected to the injection system. The injection system consists of a reciprocating air compressor, calibrated orifice plate and cubic air manifold box which has three pipes, of 25.4 mm diameter each, one inlet and two outlets. Thus the injected air passes through the two outlets to the test model and emerges from it as air jets through the blowing holes.

The Measuring Techniques:

The set up has been provided with suitable measuring devices. The measurements include velocity profiles, pressure distribution, flow rates and local skin friction coefficients. The velocity profiles measurements were carried out with flattened pitot-probe shown in Fig. (2) of 0.6 mm outlet height was held in a traversing mechanism. The traversing mechanism has a micrometer screw of a least scale count of 0.005 mm. The wall static pressure distribution measurements were carried out using the static pressure taps which were connected to an inclined multi manometer. The local skin friction coefficient measurements were carried out using Preston tube of 0.75 mm external diameter and diameter ratio of 0.6 shown in Fig. (3). The front portion of the tube was manufactured from stainless steel and stem from brass. Studies on Preston tube calibration and performance in pressure gradients were carried out by many authors [7-9]. Preston [7], based on dimensional analysis, suggested correlation of the experimental data in the form:

$$x^* = F(y^*) \quad (1)$$

where x^* and y^* are the dimensionless skin friction (τ_o) and the Preston tube reading (ΔP) given by:

$$x^* = \log(\tau_o d^2 / 4\rho v^2) \text{ and } y^* = \log(\Delta P d^2 / 4\rho v^2) \quad (2)$$

where d is the outer tube diameter.

Brown, et al. [9] calibrated Preston tube, in favourable and adverse pressure gradients, and obtained the following relationships:

$$i) \quad y^* = x^*/2 + 0.037 \quad ; \quad u_\tau d / 2\nu < 5.6 \quad (3)$$

$$ii) \quad y^* = 0.8287 - 0.1381 x^* + 0.1437 x^{*2} - 0.006 x^{*3}, \quad 5.6 < u_\tau d / 2\nu < 55 \quad (4)$$

$$\text{iii) } x^* = y^* + 2 \log (1.94 y^* + 4.1) ; 55 < u_{\tau} d / 2\nu < 800 \quad (5)$$

Patel [8] related the error, in the measured wall shear stress (τ_0), to a pressure parameter (Δ) defined as:

$$\Delta = (\nu / \rho u_{\tau}^3) (dp/dx) \quad (6)$$

The limiting values of this parameter were as follows

i) For adverse pressure gradients:

maximum error of 3% for $0 < \Delta < 0.01$, $u_{\tau} d / \nu \leq 200$
maximum error of 6% for $0 < \Delta < 0.015$, $u_{\tau} d / \nu \leq 250$

ii) For favourable pressure gradients:

maximum error 3% for $0 > \Delta > -0.005$, $u_{\tau} \cdot d / \nu \leq 200$
maximum error 6% for $0 > \Delta > -0.007$, $u_{\tau} \cdot d / \nu \leq 200$

The relationships (3-5) have been used in the present wall shear stress measurements and the effects of pressure gradient were taken into account. The injected air volume flow rate (\dot{Q}) was measured using a calibrated orifice meter. then the injected air velocity (V) was determined as: $V = \dot{Q} / (n\pi d_h^2 / 4)$ (7)

DIMENSIONAL ANALYSIS:

In order to correlate the experimental results, a dimensional analysis of the problem has been carried out. It is expected that both the wall static pressure and shear stress, in two dimensional incompressible isothermal flow with injection of same medium at the beginning of the wake, will depend on three different types of parameters. The first type of parameters represents the fluid physical properties such as the density (ρ), viscosity (μ). In the second one the parameters are related to flow conditions such as: the main flow velocity (u_{∞}) and injection flow velocity (V). The third type of parameters relate to the geometry of plate such as the: length (L), the width (w), height (H), roughness (ϵ), distance measured along the wall (x). Thus the difference between the pressure at any point on the wall (x) and a reference pressure can be written as $\Delta P = F(u_{\infty}, V, \mu, \rho, x, L, \text{ geometries})$. Using Buckingham's π theorem [11] and for constant geometries in the test section, the following relation is obtained:

$$c_p = \frac{\Delta P}{0.5 \rho u_{\infty}^2} = F' \left(\frac{1}{Re_{\infty}}, \lambda, \frac{x}{L} \right) \quad (8)$$

where c_p is the pressure coefficient, Re_{∞} is the flow Reynolds number, λ is the velocity ratio $= (V/u_{\infty})$ and x/L is the dimensionless distance from a reference point at edge of the plate then for a constant Reynolds number, the relationship (8) reduces to

$$c_p = F'' \left(\frac{x}{L}, \lambda \right) \quad (9)$$

Similarly, the following relation is obtained for the skin friction coefficient:

$$c_f = F''' \left(\frac{x}{L}, \lambda \right) \quad (10)$$

The above results (9-10) were used in correlating both the pressure and skin friction experimental results.

RESULTS AND DISCUSSION

Velocity Profiles:

The profiles of the mean velocity component in streamwise directions $u(y)$ were measured at the stations $\bar{x} = x/L = 0.12, 0.19, 0.3, 0.39, 0.48, 0.57, 0.66, 0.77$ and 0.87 for $Re = 1.8 \times 10^5$ and injection velocity ratios $\lambda = V/u_\infty = 0, 0.3, \text{ and } 0.5$. The position x is measured from a point on the wall at 88 mm . downstream of the trailing edge. To discuss the parameters which describe the velocity profiles, the sketch of velocity profile shown in Fig.(4) can be used. In the sketch the velocity profiles has been divided into two layers: i) The inner layer, which starts from zero velocity at the wall to maximum velocity (u_e), ii) outer layer (interaction zone), which starts from the maximum velocity in the profile to the wake centerline where the velocity has a minimum value (u_c). Fig.(5-A) shows the dimensionless mean velocity profiles at the positions of measurements for zero injection ratio. The interaction between the wall-boundary layer and the wake generated behind the thick plate is noticed in the experimental results. For certain velocity ratio by moving downstream from the trailing edge of the plate the wake decays while the boundary layer grows. Also, the position of maximum velocity (u_e) moves into the inner layer, the wake depth decreases and the wake width increases. Figs.(5-B) & (5-C) show the mean velocity profiles at different positions in the direction of the flow for injection velocity ratios $\lambda = V/u_\infty = 0.3$ and 0.5 . The Figures show that, for the same distance from the trailing edge of the plate, an increase of velocity ratio (λ) leads to an increase in injected mass flow rates, therefore the wake centerline velocity increases and wake depth decreases. Also the position of maximum velocity (u_e) moves into the inner layer, hence the wake width increases. It can be observed also that the rate of wake decay increases as compared with the case of zero injection velocity ratio. Fig.(6) shows the effect of injection on wake depth (B). The Figure shows that the wake depth decreases instreamwise direction for the same velocity ratio. Also. It can be seen that the wake region decreases as the velocity ratio (λ) increases. For example wake decay occurs at $x/L = 0.58, 0.52$ and 0.47 for $\lambda = 0, 0.3$ and 0.5 respectively. Fig. (7) shows (b/H) vs. x/L . From the Figure it can be observed that the wake width increases instreamwise direction, for the same velocity ratio (λ). Also, at certain distance as the velocity ratio increases the wake width increases.

Wall Static Pressure Results:

Fig(8.) shows the variation of the static pressure coefficient (cp) along the wall of the test section at $Re_\infty = 1.8 \times 10^5$. For different velocity ratios it can be noticed that the static pressure increases instreamwise direction. This increase in pressure could be due to the effect of increasing the cross section area of flow after the blocking of the thick plate. It can be observed also that the wall static pressure coefficient (cp) decreases by increasing the velocity ratio (λ) because of inertia of fluid added from blowing to the flow.

Skin Friction Results:

Fig. (9) shows the variation of skin friction coefficient (cf) along the wall of the test section for $Re_{\infty} = 1.8 \times 10^5$ at different velocity ratios. It can be observed that the skin friction coefficient decreases as the distance (x/L) increases for constant (λ). Also the rate of decrease of cf is relatively high in the region of wake decay. In the second region the skin friction coefficient is still decreasing, but at a smaller rate and approaching a constant value. The figure shows that as the velocity ratio increases the skin friction coefficient increases at any distance i.e. as velocity ratio increases the flow becomes more stable against separation.

Boundary Layer Integral Parameters:

Two important boundary layer integral parameters, which are the shape factor (H_{12}) and the momentum thickness Reynolds number Re_{δ_2} were evaluated from measured velocity profiles and presented in Figs. (10) and (11). Fig. (10) shows the variation of shape factor (H_{12}) with distance (x/L) for different velocity ratios (λ). From the Figure it can be noticed that (H_{12}) decreases slightly in stream wise direction. It can be observed also that the shape factor decreases due to the increase of velocity ratio (λ). Thus no flow separation can occur here because the value of H is less than 1.8 which is often used to specify the onset of flow separation [10] everywhere. Fig. (11) shows the variation of Reynolds number Re_{δ_2} vs. x/L at different velocity ratios. It can be seen that (Re_{δ_2}) decreases due to increase of velocity ratio (λ).

CONCLUSIONS

This paper presents an experimental study of the turbulent wake-boundary layer interaction with injection at wake beginning. The results of the study leads to the following conclusions:

1. For constant injection to main stream velocity ratio, moving downstream from the wake beginning, the wake decays, while the boundary layer grows. Also the wake depth decreases, the wake width increases and the position of maximum velocity moves into the inner layer.
2. At a certain distance from wake beginning as the velocity ratio increases, the rate of wake decay increases, the wake centerline velocity increases and the wake width increase while the wake depth decreases.
3. The wall static pressure coefficient increases slightly as a result of increasing the cross section area of flow after the blocking of the thick plate and decreases with increasing velocity ratio because of inertia of fluid added from blowing to the flow.
4. The skin friction coefficient decreases in the direction of mainstream and increases as a result of increasing velocity ratio.
5. Both shape factor and momentum Reynolds number decreases as the velocity ratio increases.

REFERENCES

- [1] Dedoussis V., G. Bergeles and N. Athanassiadis, "An experimental investigation of the turbulent wake of a thin flat plate" The Fourth International Conference for Mechanical Power Engineering, Faculty of Engineering, Cairo University V-59 October, 1982.
- [2] Heikal H.A., S.S. Ayad, H.M. Helmy and A.M. Osman, "Experimental study of the plane turbulent wake behind an aerofoil with pressure gradient" 4th International Conference for Mechanical Power Engineering, Ain Shams University, V.3, P. 14, 13-15 October, 1984.
- [3] Heikal H.A., S.K. El-Dandoush, M.M.M. El-Telbany, H.A.A. El-Gabry and M.F. Abd-Rabbo, "Turbulent wake behind aerofoil with pressure gradient effect" The Fourth international conference for Mechanical Power Engineering, October, 1982, Faculty of Engineering, Cairo University, V.5
- [4] Change K.C., M.N. Bui, T. Cebeci and J.H. Whitelaw " The calculation of turbulent wakes" AIAA Journal vol. 24, No.2, pp. 200-201, February, 1986.
- [5] Zacharias A., "An experimental and theoretical investigation of the interaction between the engine jet and surrounding flow field with regard to the pressure drag on after bodies" Advisory Group for Aerospace Research and Development Conference Proceedings No. 308, fluid Dynamics of Jets with applications to V/stol pp. 8-1 November, 1981.
- [6] Hoch.j., and L.M. Jiji, "Two dimensional turbulent offset jet boundary interaction" Journal of fluids Engineering Vol. 103, PP. 154-161, March, 1981.
- [7] Preston, J.H., "The determination of turbulent skin friction by means of pitot tubes", Journal of Royal Aeronautical Society Vol. 58, PP. 102-121, February 1954.
- [8] Patel, V.C., "Calibration of Preston tube and limitations on its uses in pressure gradient", Journal fluid Mech., Vol. 23, Part 1, pP. 185-208, 1965.
- [9] Brown, K.C., and P.N. Joubort, "The measurement of skin friction in turbulent boundary layers with adverse pressure gradient" J. fluid Mech., 1969, Vol.35, Part 4, PP. 737-757.
- [10] Cebeci, T., G.T. Mosinskis and A.M.O. Smith, " Calculation of separation points in In Compressible Turblent Flows" J. Aircraft, Vol 9, No. 9, PP. 618-624, September, 1972.
- [11] Kenneth, J. "Kent's mechanical Engineering hand book" 12th ed., TOPPAN Company, LTD, Japan, 1950.

NOMECLATURE

B;b : wake depth (m); Half wake width (m)
 cd;cf;cp: Discharge coefficient₂ of orifice; skin friction coefficient ($cf = (\tau_o / 0.5\rho u_\infty^2)$); wall static pressure coefficient ($cp = (P - Pr) / 0.5\rho u_\infty^2$).
 d; d_h; d⁺: Preston-tube external diameter (m); diameter of the hole at the trailing edge's test model; dimensionless parameter ($d^+ = u_\tau d / \nu$).

- H; H_{12} : Half test section height; shape factor ($H_{12} = \delta_1/\delta_2$)
- L : Plate length, (m)
- n : The number of holes at the trailing edge of the test section.
- P; P_r ; P_t : Static; reference static; total pressures (N/m^2).
- ΔP : The difference between the Preston tube reading and the wall static pressure.
- Q' : Volume flow rate for injected air (m^3/sec).
- Re_∞ : Reynolds number based upon test section height and free stream velocity $Re_\infty = (u_\infty \cdot 2H)/\nu$.
- Re_{δ_2} : Reynolds number based upon local momentum thickness and maximum velocity ($Re_{\delta_2} = Ue \delta_2/\nu$).
- u_c ; u_e ; u_∞ ; u_t : Velocity at the wake centerline; maximum velocity free stream velocity; friction velocity ($u_t = \sqrt{\tau_o/\rho_o}$)
- V : Injection velocity.
- w : width of the plate.
- x; x^* : Distance measured along the wall downstream of the trailing edge of the plate; dimensionless skin friction parameter.
- y; y^* : Distance normal to the wall of the test section (m); Dimensionless Preston tube reading.
- Δ ; δ ; δ_1 ; δ_2 : Pressure gradient parameter ($\Delta = (\nu/\rho u_t^3) (dp/dx)$), boundary layer thickness; boundary layer displacement thickness ($\delta_1 = \int_0^\delta (1-u/u_e) dy$); momentum thickness ($\delta_2 = \int_0^\delta (u/u_e) (1-u/u_e) dy$)
- ϵ ; λ ; μ ; ν ; ρ ; τ_o : Plate roughness; velocity ratio; Dynamic viscosity ($N.S/m^2$); kinematic viscosity (m^2/S); density (kg/m^3); wall shear stress.

SUBSCRIPTS:

- o : Condition at wall surface.
- r : Condition at reference position.
- ∞ : Condition at free stream velocity.
- e : Condition at maximum velocity.

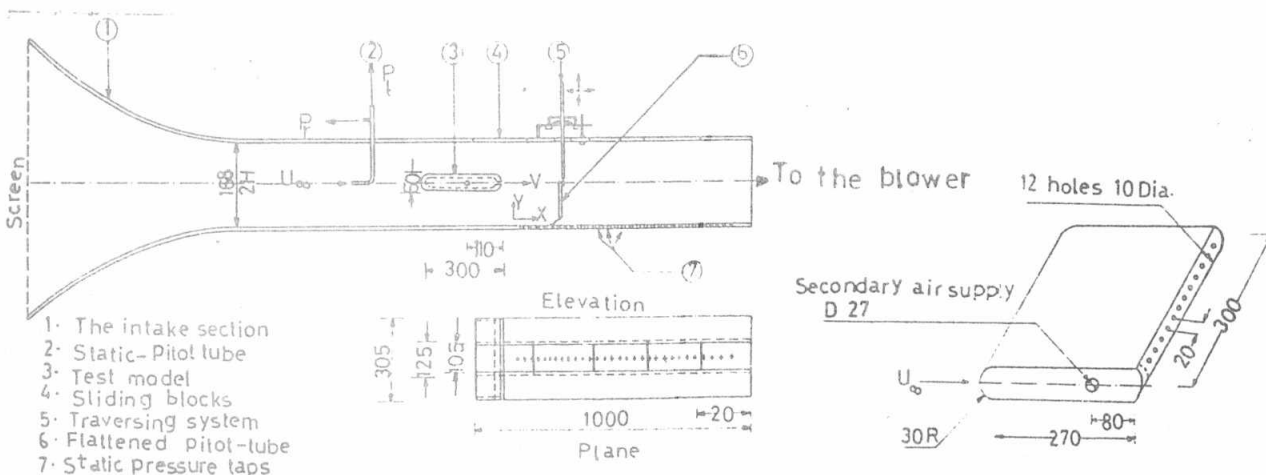


FIG. (1) Diagrammatic sketch of tunnel working section and the model . DIM: in MMS

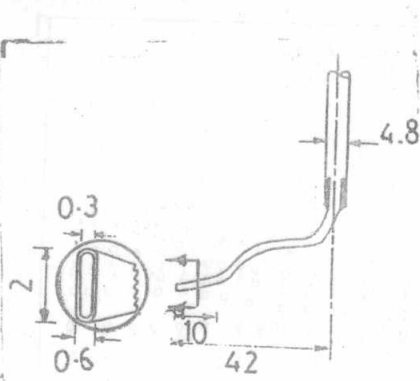


Fig. (2): Flattened Pitot-tube

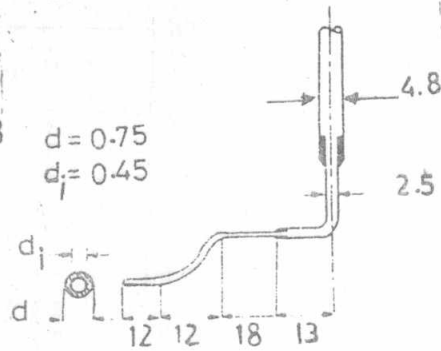


Fig. (3): Preston-tube

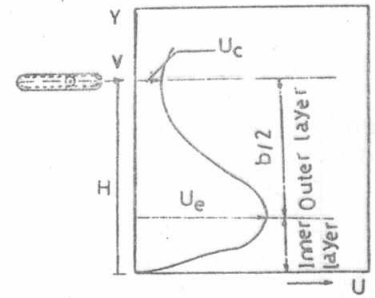


Fig. (4): Representative sketch of velocity profile.

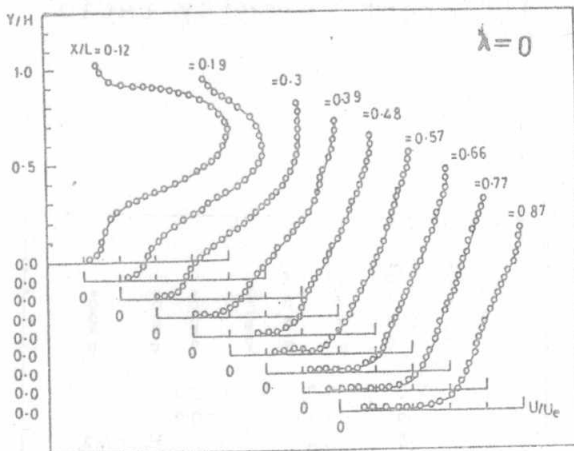


Fig. (5-A)

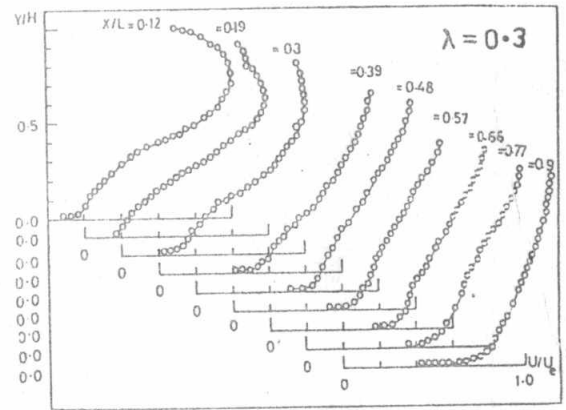


Fig. (5-B)

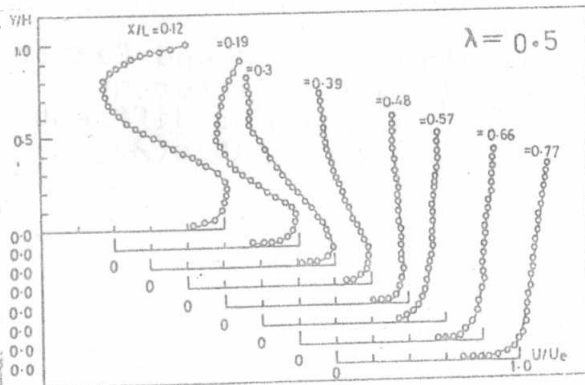


Fig. (5-C)

Fig. (5): Measured velocity Distributions at different position ($\bar{x} = x/L$) and constant Reynolds number with different velocity ratio (λ), A: $\lambda = 0$, B: $\lambda = 0.3$, & C: $\lambda = 0.5$.

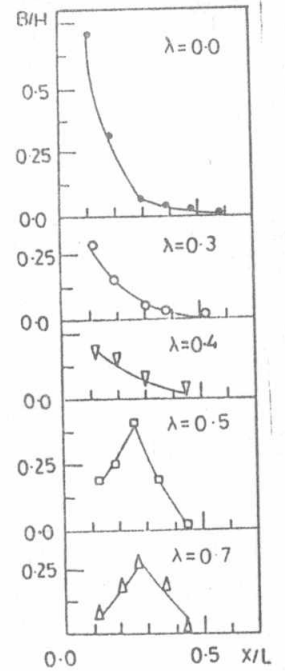


Fig. (6): Effect of velocity ratio (λ) on wake depth (B)

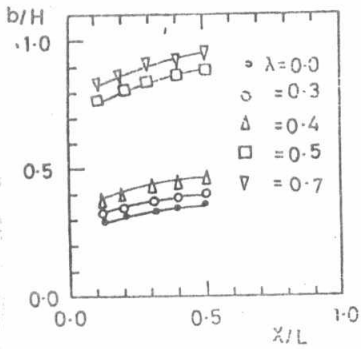


Fig. (7): Effect of velocity ratio (λ) on wake width (b)

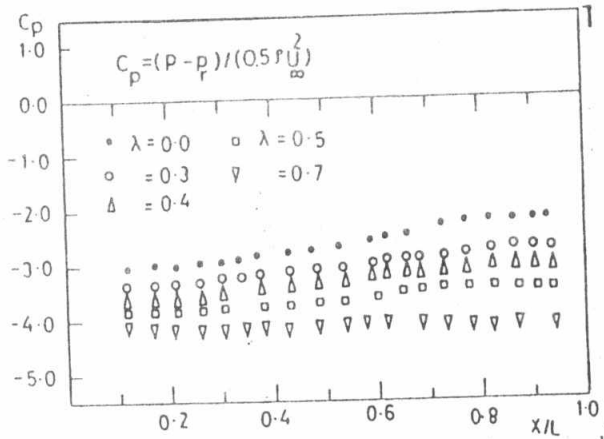


Fig. (8): Measured wall pressure distribution (C_p) at different velocity ratio (λ).

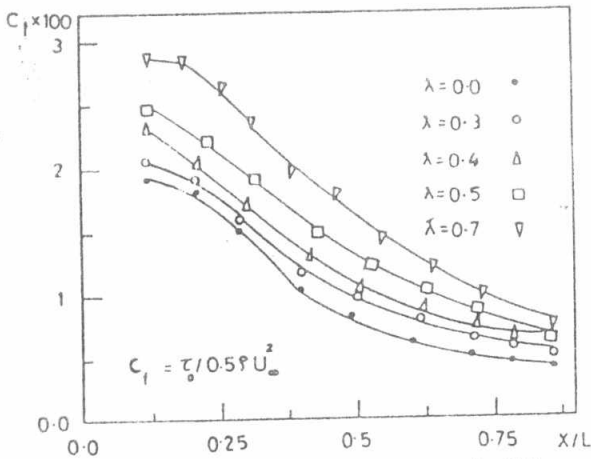


Fig. (9): Effect of Velocity ratio (λ) on the skin friction coefficient

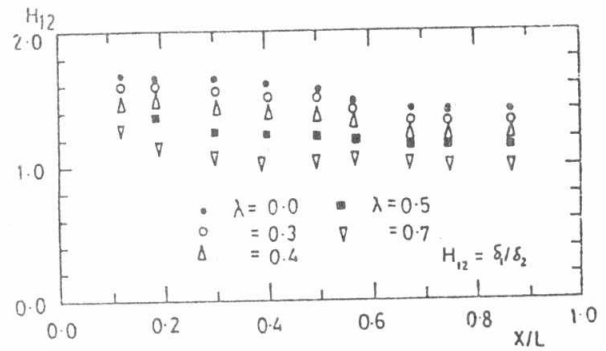


Fig. (10): Evaluated shape factor (H_{12}) at different position for different velocity ratio (λ)

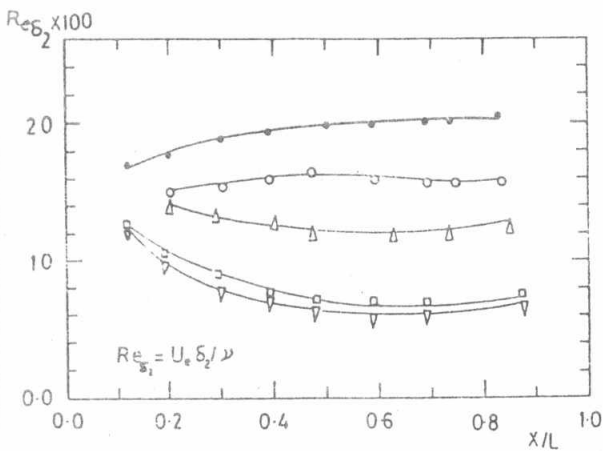


Fig. (11): Evaluated momentum Reynolds number for different velocity ratio (λ).